Figure S1

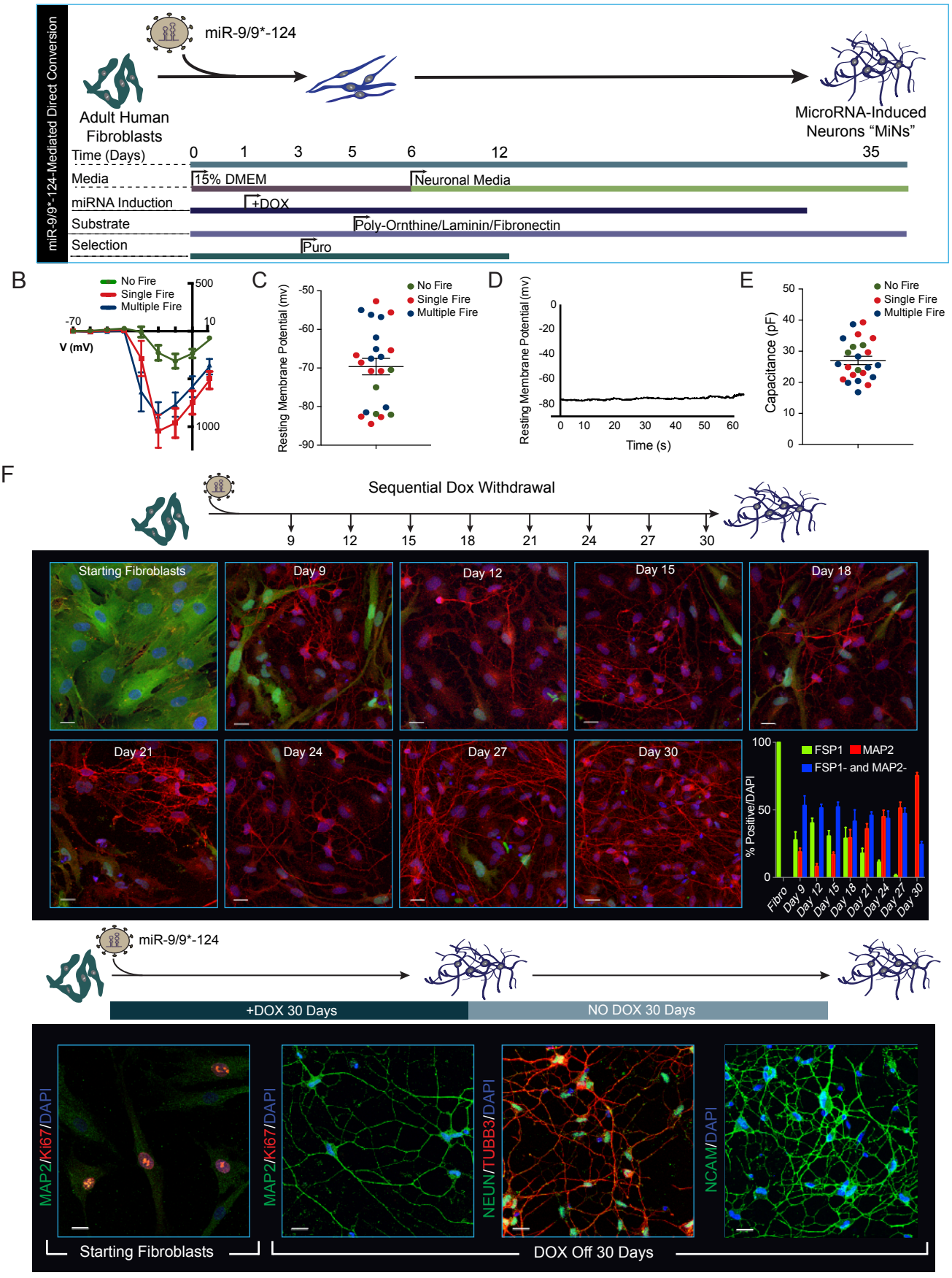
A
miR-9/9*-124-Mediated Direct Conversion
miR-9/9*-124
Adult Human Fibroblasts
MicroRNA-Induced Neurons "MiNs"
Time (Days)
0 1 3 5 6 12 35
Media
15% DMEM
Neuronal Media
miRNA Induction
+DOX
Substrate
Poly-Ornthine/Laminin/Fibronectin
Selection
Puro
B
No Fire
Single Fire
Multiple Fire
V (mV)
C
Resting Membrane Potential (mv)
D
Time (s)
E
Capacitance (pF)
F
Sequential Dox Withdrawal
9 12 15 18 21 24 27 30
Starting Fibroblasts
Day 9
Day 12
Day 15
Day 18
Day 21
Day 24
Day 27
Day 30
FSP1
MAP2
FSP1- and MAP2-
% Positive/DAPI
Fibro
G
miR-9/9*-124
+DOX 30 Days
NO DOX 30 Days
MAP2/Ki67/DAPI
NEUN/TUBB3/DAPI
NCAM/DAPI
Starting Fibroblasts
DOX Off 30 Days

Figure S2

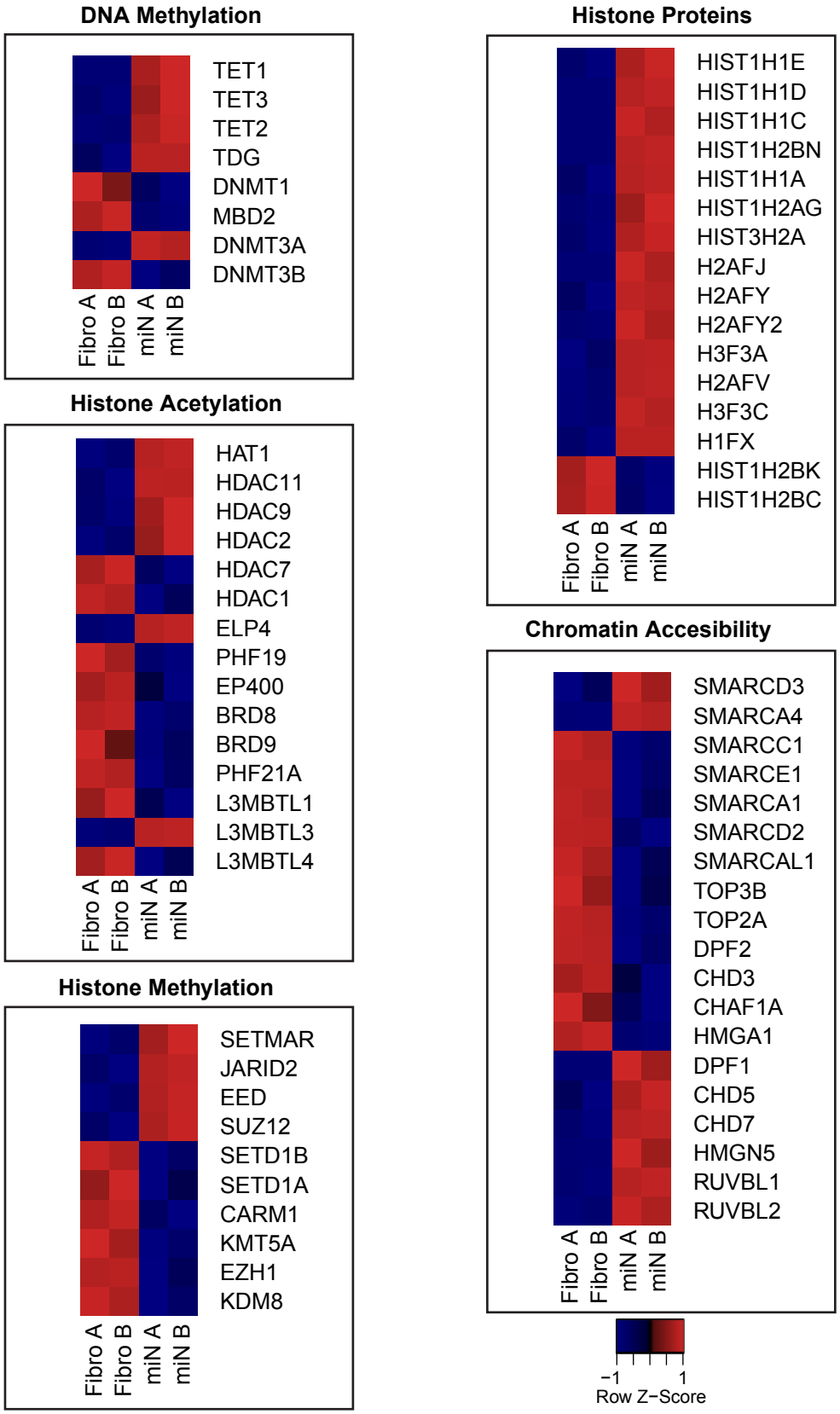
DNA Methylation
TET1
TET3
TET2
TDG
DNMT1
MBD2
DNMT3A
DNMT3B
Fibro A
Fibro B
miN A
miN B
Histone Acetylation
HAT1
HDAC11
HDAC9
HDAC2
HDAC7
HDAC1
ELP4
PHF19
EP400
BRD8
BRD9
PHF21A
L3MBTL1
L3MBTL3
L3MBTL4
Fibro A
Fibro B
miN A
miN B
Histone Methylation
SETMAR
JARID2
EED
SUZ12
SETD1B
SETD1A
CARM1
KMT5A
EZH1
KDM8
Fibro A
Fibro B
miN A
miN B
Histone Proteins
HIST1H1E
HIST1H1D
HIST1H1C
HIST1H2BN
HIST1H1A
HIST1H2AG
HIST3H2A
H2AFJ
H2AFY
H2AFY2
H3F3A
H2AFV
H3F3C
H1FX
HIST1H2BK
HIST1H2BC
Fibro A
Fibro B
miN A
miN B
Chromatin Accesibility
SMARCD3
SMARCA4
SMARCC1
SMARCE1
SMARCA1
SMARCD2
SMARCAL1
TOP3B
TOP2A
DPF2
CHD3
CHAF1A
HMGA1
DPF1
CHD5
CHD7
HMGN5
RUVBL1
RUVBL2
Fibro A
Fibro B
miN A
miN B
−1
1
Row Z−Score

Figure S3

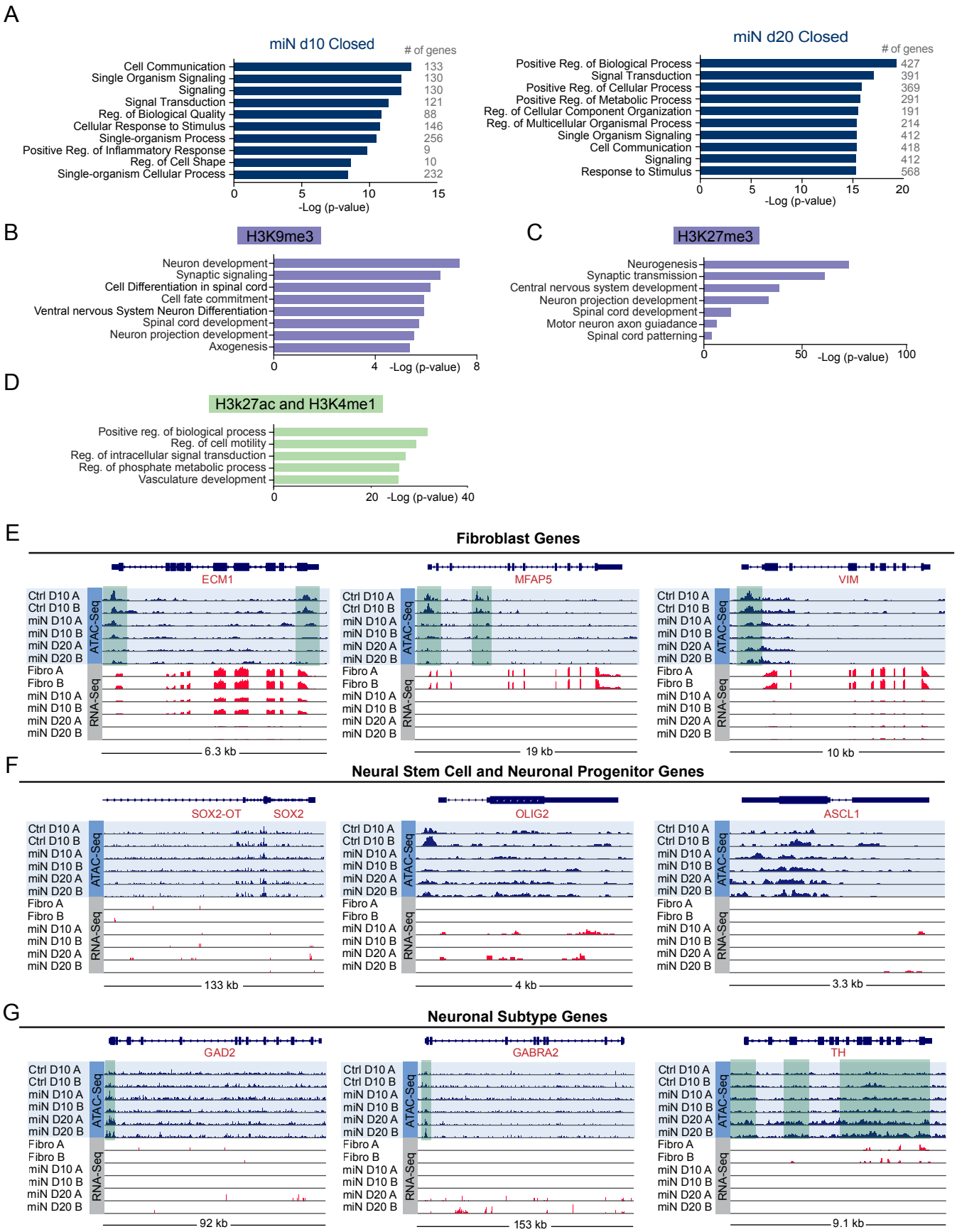
A
miN d10 Closed
# of genes
Cell Communication 133
Single Organism Signaling 130
Signaling 130
Signal Transduction 121
Reg. of Biological Quality 88
Cellular Response to Stimulus 146
Single-organism Process 256
Positive Reg. of Inflammatory Response 9
Reg. of Cell Shape 10
Single-organism Cellular Process 232
0 5 10 15
-Log (p-value)
miN d20 Closed
# of genes
Positive Reg. of Biological Process 427
Signal Transduction 391
Positive Reg. of Cellular Process 369
Positive Reg. of Metabolic Process 291
Reg. of Cellular Component Organization 191
Reg. of Multicellular Organismal Process 214
Single Organism Signaling 412
Cell Communication 418
Signaling 412
Response to Stimulus 568
0 5 10 15 20
-Log (p-value)
B
H3K9me3
Neuron development
Synaptic signaling
Cell Differentiation in spinal cord
Cell fate commitment
Ventral nervous System Neuron Differentiation
Spinal cord development
Neuron projection development
Axogenesis
0 4 8
-Log (p-value)
C
H3K27me3
Neurogenesis
Synaptic transmission
Central nervous system development
Neuron projection development
Spinal cord development
Motor neuron axon guiadance
Spinal cord patterning
0 50 100
-Log (p-value)
D
H3k27ac and H3K4me1
Positive reg. of biological process
Reg. of cell motility
Reg. of intracellular signal transduction
Reg. of phosphate metabolic process
Vasculature development
0 20 40
-Log (p-value)
E
Fibroblast Genes
ECM1
MFAP5
VIM
Ctrl D10 A
Ctrl D10 B
miN D10 A
miN D10 B
miN D20 A
miN D20 B
Fibro A
Fibro B
ATAC-Seq
RNA-Seq
6.3 kb
19 kb
10 kb
F
Neural Stem Cell and Neuronal Progenitor Genes
SOX2-OT
SOX2
OLIG2
ASCL1
133 kb
4 kb
3.3 kb
G
Neuronal Subtype Genes
GAD2
GABRA2
TH
92 kb
153 kb
9.1 kb

Figure S4

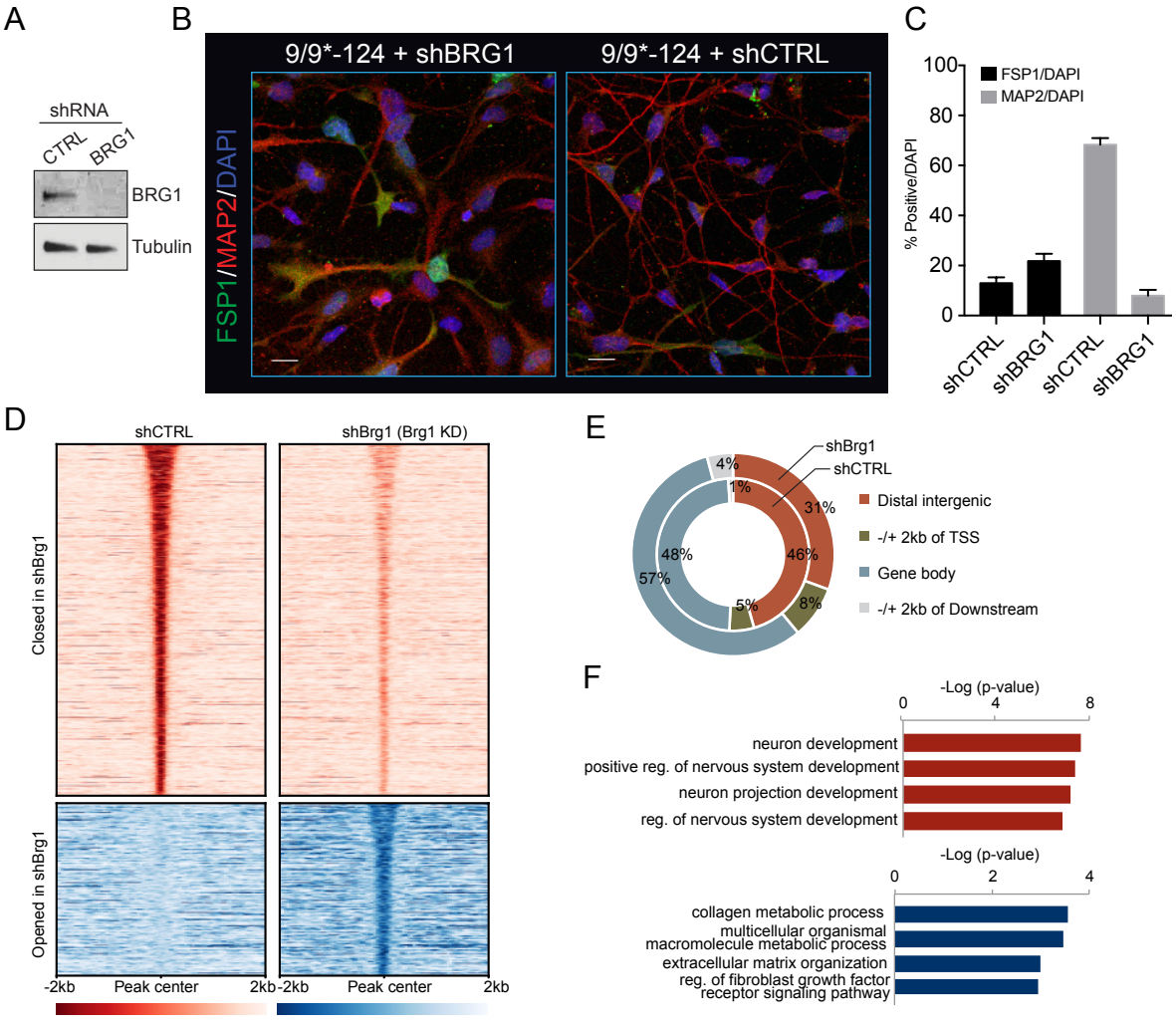
A
shRNA
CTRL
BRG1
BRG1
Tubulin
B
9/9*-124 + shBRG1
9/9*-124 + shCTRL
FSP1/MAP2/DAPI
C
FSP1/DAPI
MAP2/DAPI
% Positive/DAPI
100
80
60
40
20
0
shCTRL
shBRG1
shCTRL
shBRG1
D
shCTRL
shBrg1 (Brg1 KD)
Closed in shBrg1
Opened in shBrg1
-2kb
Peak center
2kb
-2kb
Peak center
2kb
E
shBrg1
shCTRL
4%
1%
31%
46%
48%
57%
5%
8%
Distal intergenic
-/+ 2kb of TSS
Gene body
-/+ 2kb of Downstream
F
-Log (p-value)
0
4
8
neuron development
positive reg. of nervous system development
neuron projection development
reg. of nervous system development
-Log (p-value)
0
2
4
collagen metabolic process
multicellular organismal macromolecule metabolic process
extracellular matrix organization
reg. of fibroblast growth factor receptor signaling pathway

Figure S5

A

TF's Tested with miR-9/9*-124

ISL1	NGN2 OLIG2 RXRG RARβ
LHX3a	NGN2 RXRG RARβ
ISL1 LHX3a	NKX 2.2
ND2	NKX 6.2
NGN2	NKX 6.2 Isl1
NGN2 ISL1	NKX 6.2 LHX3a
NGN2 ISL1 RXRG RARβ	OLIG2
NGN2 LHX3a	OLIG2 ISL1
NGN2 LHX3a ISL1	OLIG2 LHX3a
NGN2 LHX3a ISL1 RXRG RARβ	OLIG2 NKX 6.2
NGN2 LHX3a RXRG RARβ	OLIG2 NKX 6.2 RXRG RARβ
NGN2 OLIG2	OLIG2 NKX6.2 ISL1
NGN2 OLIG2 ISL1	RXRG RARβ
NGN2 OLIG2 ISL1 RXRG RARβ	

B

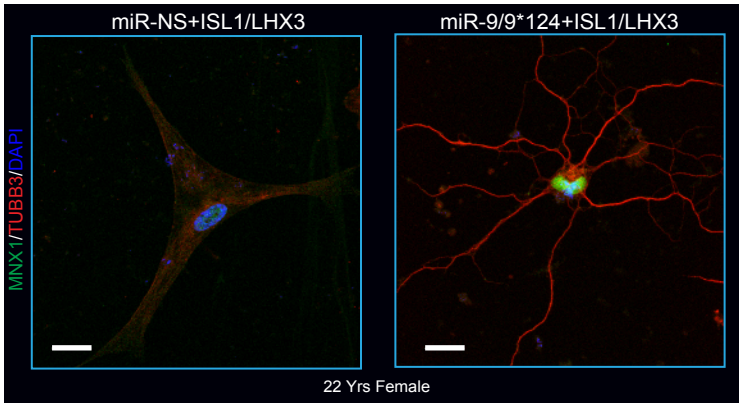

C

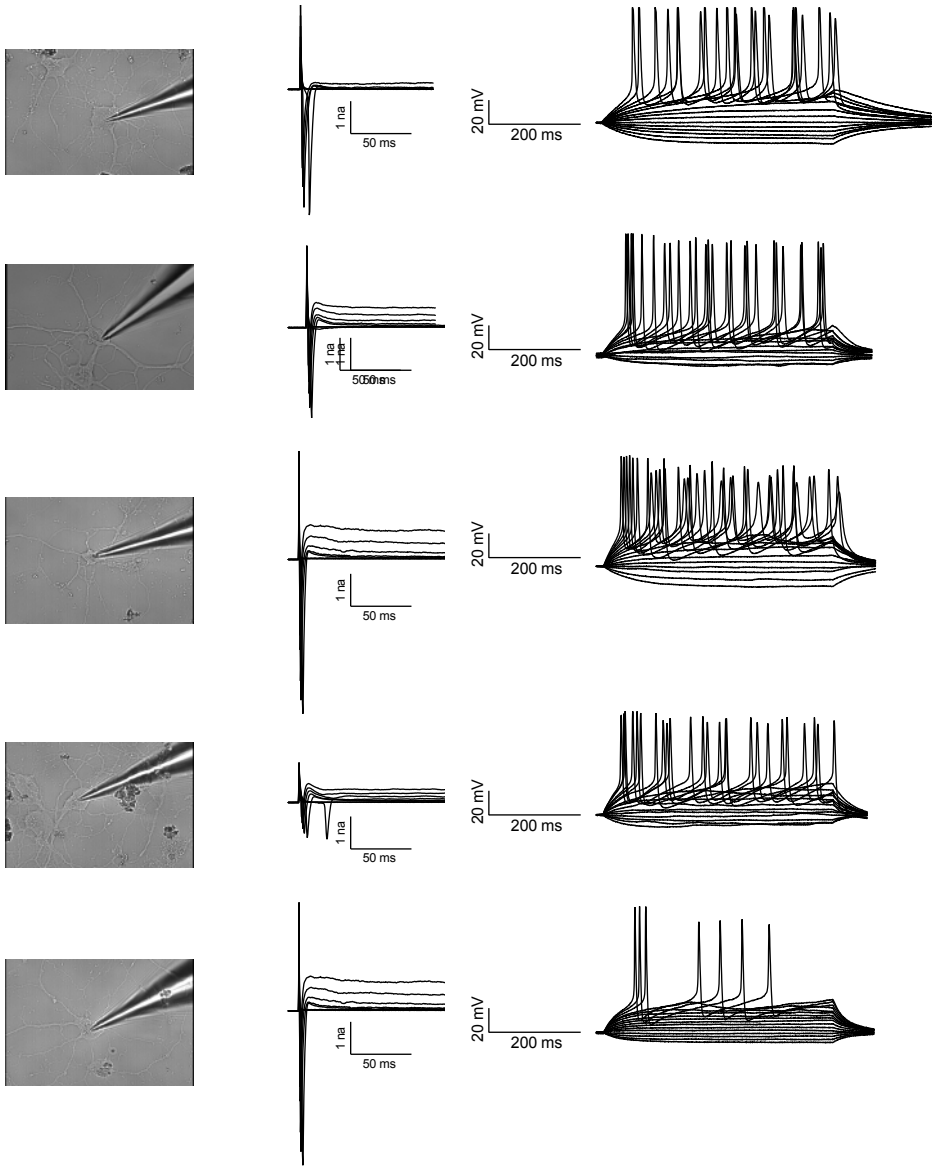

Figure S6

A

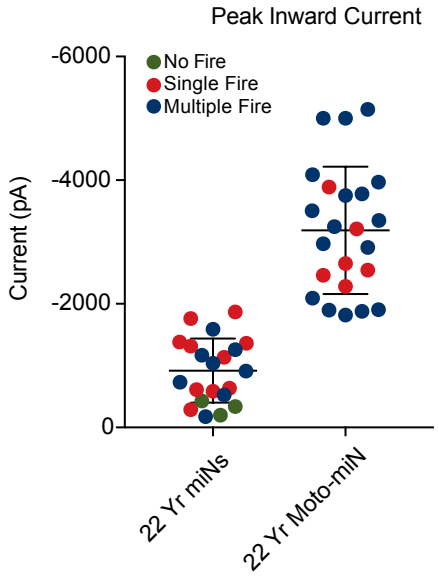

B

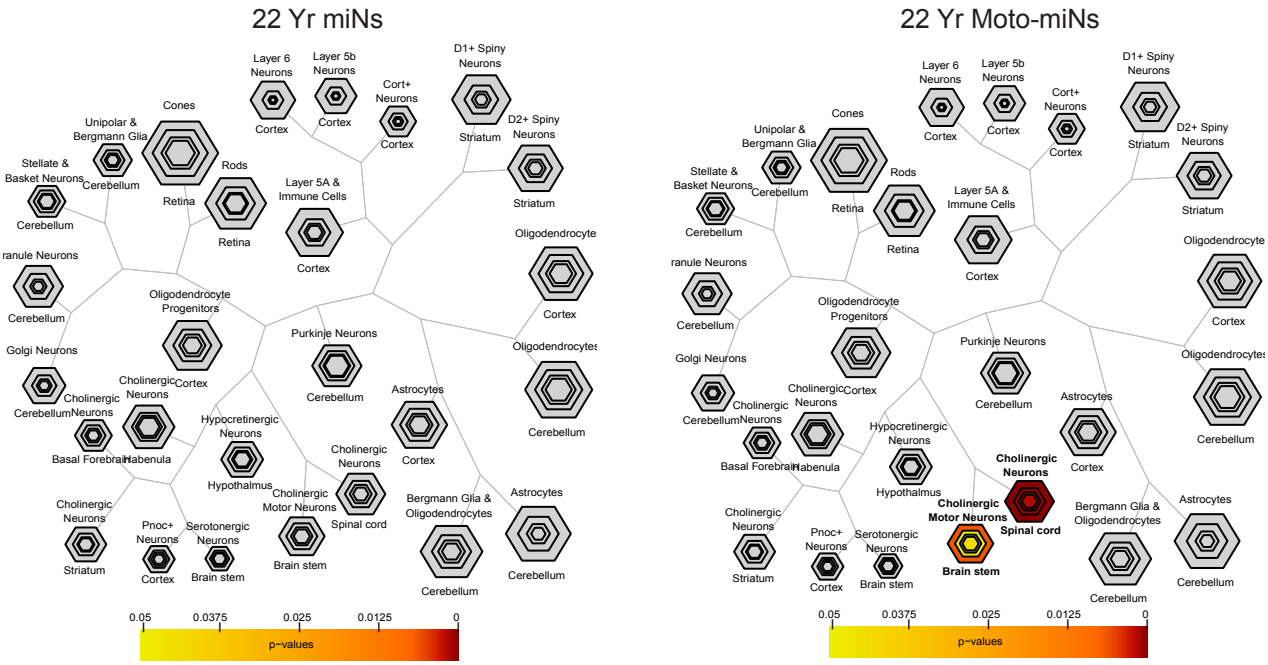

C

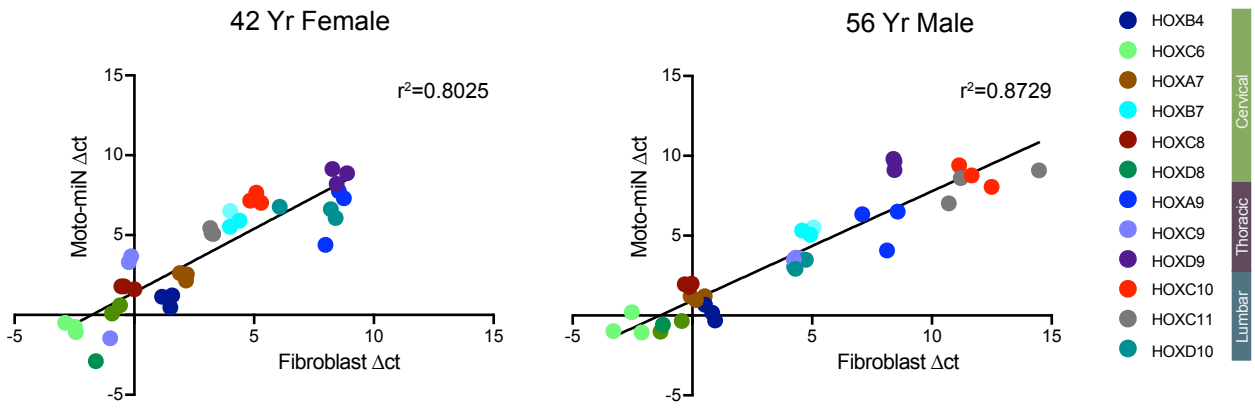

Figure S7

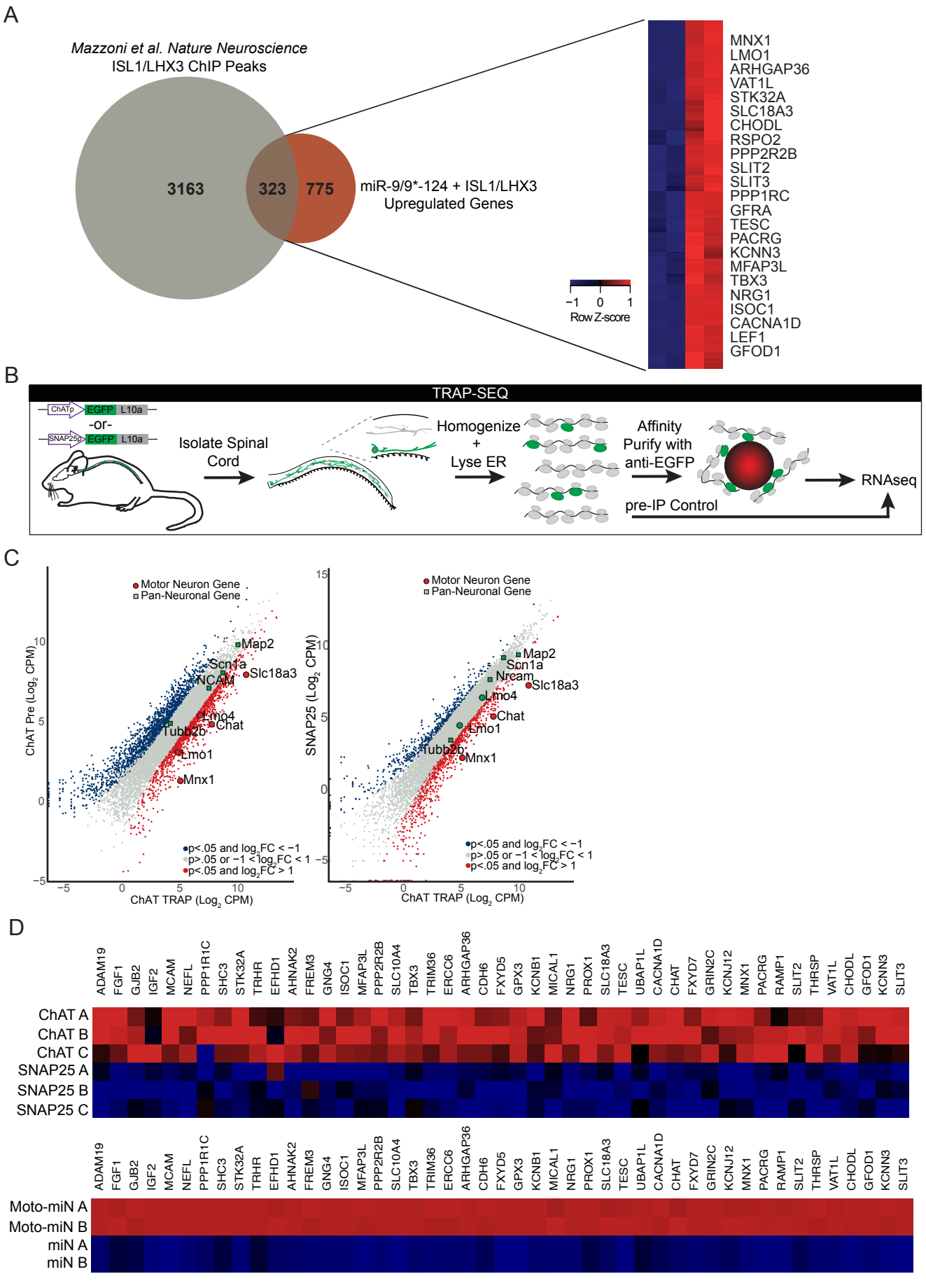
A
Mazzoni et al. Nature Neuroscience
ISL1/LHX3 ChIP Peaks
3163
323
775
miR-9/9*-124 + ISL1/LHX3
Upregulated Genes
Row Z-score
MNX1
LMO1
ARHGAP36
VAT1L
STK32A
SLC18A3
CHODL
RSPO2
PPP2R2B
SLIT2
SLIT3
PPP1RC
GFRA
TESC
PACRG
KCNN3
MFAP3L
TBX3
NRG1
ISOC1
CACNA1D
LEF1
GFOD1
B
TRAP-SEQ
ChATp
EGFP
L10a
-or-
SNAP25p
Isolate Spinal
Cord
Homogenize
+
Lyse ER
Affinity
Purify with
anti-EGFP
RNAseq
pre-IP Control
C
Motor Neuron Gene
Pan-Neuronal Gene
ChAT Pre (Log2 CPM)
ChAT TRAP (Log2 CPM)
Map2
Scn1a
NCAM
Slc18a3
Lmo4
Chat
Tubb2b
Lmo1
Mnx1
p<.05 and log2FC < −1
p>.05 or −1 < log2FC < 1
p<.05 and log2FC > 1
SNAP25 (Log2 CPM)
Ncam
D
ADAM19
FGF1
GJB2
IGF2
MCAM
NEFL
PPP1R1C
SHC3
STK32A
TRHR
EFHD1
AHNAK2
FREM3
GNG4
ISOC1
MFAP3L
PPP2R2B
SLC10A4
TBX3
TRIM36
ERCC6
ARHGAP36
CDH6
FXYD5
GPX3
KCNB1
MICAL1
NRG1
PROX1
SLC18A3
TESC
UBAP1L
CACNA1D
CHAT
FXYD7
GRIN2C
KCNJ12
MNX1
PACRG
RAMP1
SLIT2
THRSP
VAT1L
CHODL
GFOD1
KCNN3
SLIT3
ChAT A
ChAT B
ChAT C
SNAP25 A
SNAP25 B
SNAP25 C
Moto-miN A
Moto-miN B
miN A
miN B

Figure S1, Related to Figure 1

MiRNA-Mediated Conversion into Neuronal Fate is Stable
(A) Detailed schematic of miR-9/9*-124 direct conversion protocol.
(B) Combined plot of the current (I) - voltage (V) relationship for all neurons recorded.
(C) Tabulated values of resting membrane potentials in miNs.
(D) Gap-free recording of resting membrane potential in a miN.
(E) Tabulated values of capacitance values in miNs.
(F) MiR-9/9*-124 was ectopically expressed under a doxycycline (DOX) inducible promoter in 22 year old human fibroblasts for 9 days then DOX was removed from the media at 3 day intervals. Cells were cultured until reprogramming day 30. Neuronal fate was assayed by immunostaining for the pan-neuronal marker MAP2 and the fibroblast identity was determined by FSP1 expression. Scale bar = 20μm. All data are represented as mean ± SEM.
(G) MiR-9/9*-124 was ectopically expressed under a DOX-inducible promoter in 22 year old human fibroblasts for 30 days then DOX was removed from the media and cells were cultured for an additional 30 days. Stable adoption of the neuronal fate was assayed by immunostaining for the pan-neuronal markers MAP2, NEUN, TUBB3 and NCAM. To assay if cells remained post-mitotic cells were stained with the proliferative marker ki-67. Scale bar = 20μm.
All data are represented as mean ± SEM.

Figure S2, Related to Figure 2

Expression Changes in Epigenetic Modifiers During Reprogramming
Heatmaps show expression changes observed between miNs and fibroblasts within a subset of proteins that influence chromatin state through various modes.

Figure S3, Related to Figure 5

Pre-existing Heterochromatic Neuronal Loci Open in Response to miR-9/9*-124 Expression.
(A) Top GO terms associated with promoter regions that close during reprogramming from fibroblasts to miNs.
(B) Closed regions in fibroblasts marked by H3K9me3 that open during neuronal reprogramming are enriched for neuronal GO terms.
(C) Closed regions in fibroblasts marked by H3K27me3 that open during reprogramming are also enriched for neuronal GO terms.
(D) Pre-existing distal H3K27ac and H3K4me1 marks within fibroblasts that close during neuronal reprogramming show GO terms related to general biological processes.
(E) Genome browser snapshots demonstrating closing and loss of fibroblast gene expression (*ECM1*, *MFAP5*, and *VIM*).
(F) Genome browser snapshots demonstrating neither opening or activation of progenitor genes (*SOX2*, *OLIG2* and *ASCL1*).
(G) Genome browser snapshots demonstrating neuronal subtype gene loci that open, but do not show gene expression changes (*GAD2* and *GABRA2*, GABAergic markers; *TH*, dopaminergic neuron marker). Shaded green: location of differential ATAC peaks detected.

Figure S4, Related to Figure 5

Loss of BRG1 Prevents Neuronal Fate Acquisition
(A) BRG1 expression in human fibroblasts expressing shCTRL or shBRG1
(B) Adult human fibroblasts ectopically expressing miR-9/9*-124 and shBRG1 or shCTRL for 20 days, immunostained for the pan-neuronal marker MAP2 and fibroblast marker FSP1. Scale bars = 20μm.
(C) Quantification of (B) MAP2 and FSP1 positive cells over total number of cells (DAPI). Scoring for MAP2-positive cells, only cells with processes at least three times the length of the soma were counted. Data are represented as mean ± SEM. shBRG1 n = 155 cells, shCTRL, n = 173 cells,
(D) Heatmaps showing ATAC signal intensity in open and close chromatin peaks in shBRG1 and shCTRL. All open and closed chromatin regions were ranked according to maximum intensity across all samples.
(E) The genomic distribution of ATAC signals in cells expressing miR-9/9*-124 and shCTRL or shBRG1.
(F) GO terms showing biological function of closed (lost in shBRG1, red) and open (retained in shBRG1, blue) regions.

Figure S5, Related to Figure 6

Identification of Transcription Factors For Defining Motor Neuron Specific Conversion
(A) Candidate motor neuron transcription factors and combinations co-expressed with miR-9/9*-124 in human fibroblasts.
(B) Immunocytochemistry of adult human fibroblasts overexpressing a non-specific miRNA (miR-NS) and ISL1/LHX3 (left) or miR-9/9*-124 and ISL1/LHX3 (right) for 35 days. Images demonstrate the necessity of miR-9/9*-124 for opening the neurogenic potential of human fibroblasts. Scale bar = 20μm.
(C) Additional representative inward/outward whole-cell currents and repetitive AP waveforms generated from whole cell patch clamp recordings of Moto-miNs. Images show the patch clamped cells.

Figure S6, Related to Figure 7

Addition of ISL1/LHX3 to miR-9/9*-124 Increases Functional Maturity and Generates Motor Neuron Transcriptional Network
(A) Peak inward current measured during voltage clamp mode of miNs and Moto-miNs reveals increased peak inward current in Moto-miNs (-3,189 pA ± 214 pA) compared to miNs (-919 pA ±113 pA). Data are represented as mean ± SEM.
(B) Cell Type-specific Enrichment Analysis (CSEA) tool reveals the top 100 most significantly expressed genes in miNs do not enrich for defined neuronal subtypes (left), while the top 100 most significantly expressed genes in Moto-miNs are enriched in cholinergic motor neurons in the brain stem and spinal cord.
(C) HOX gene expression analysis by qRT-PCR in 42-year-old female and 56-year-old male donor fibroblasts before and after conversion confirms that Moto-miNs retain donor fibroblast HOX gene expression patterns. Data represent ΔCT values for each biological replicate (3 separate Moto-miN conversions).

Figure S7, Related to Figure 7

Direct Comparison of Moto-miN Transcriptome to *in vivo* Mouse Motor Neurons by Translating Ribosomal Affinity Purification (TRAP) Sequencing.

(A) Venn Diagram depicting the number of ISL1/LHX3 ChiP-seq peaks identified by *Mazzoni et al.* during ISL1/LHX3 directed ES to motor neuron differentiation (3,486) and genes enriched in Moto-miN transcriptome (775). Heatmap shows overlapping activated genes (323) include hallmark motor neuron markers.
(B) Schematic of TRAP-Seq strategy used to identify transcripts in all neurons (SNAP-25 genetic driver) and motor neurons (CHAT genetic driver) in mouse spinal cord. TRAP is a method to precipitate actively translated mRNA bound to ribosomes using an antibody to EGFP-L10A.
(C) Pairwise comparisons between mean expression values in CHAT IP v. Pre-IP (left) and CHAT IP v. SNAP25 IP (right). Differentially expressed genes are shown in red (logFC > 1 and $p < 0.05$) and blue (logFC < -1 and $p < 0.05$).
(D) Example mean expression values of overlapping genes between human (Moto-miNs versus miNs) and mouse (all spinal cord neurons SNAP25-TRAP) and motor neurons (ChAT-TRAP) datasets.

Supplemental Table 1, related to STAR Methods section. Primer sequences used for qRT PCR analysis

Primer Name	Sequence (5'-3')
S100A4 FWD	GATGAGCAACTTGGACAGCAA
S100A4 REV	CTGGGCTGCTTATCTGGGAAG
VIM FWD	AGTCCACTGAGTACCGGAGAC
VIM REV	CATTTCACGCATCTGGCGTTC
COL13A1 FWD	GGAGACGGCTATTTTGGGACG
COL13A1 REV	TCCTTGAGTGGAGCTTCCATT
ChAT FWD	TCAATCATGTCCAGCGAGTC
ChAT REV	AACGAGGACGAGCGTTTG
HB9 FWD	CTCCTACTCGTACCCGCAG
HB9 REV	TTGAAGTCGGGCATCTTAGGC
SLC18A3 FWD	TTCGCCTCTACAGTCCTGTTC
SLC18A3 REV	GCTCCTCCGGGTACTTATCG
HOXB4 FWD	CGTGAGCACGGTAAACCCC
HOXB4 REV	CGAGCGGATCTTGGTGTTG
HOXC6 FWD	ACAGACCTCAATCGCTCAGGA
HOXC6 REV	AGGGGTAAATCTGGATACTGGC
HOXA7 FWD	CGTTCCGGGCTTATACAATGT
HOXA7 REV	CTCGTCCGTCTTGTCGCAG
HOXB7 FWD	TTCCCAGAACAAACTTCTTGTGC
HOXB7 REV	GCATGTTGAAGGAACTCGGCT
HOXC8 FWD	ACCGGCCTATTACGACTGC
HOXC8 REV	TGCTGGTAGCCTGAGTTGGA
HOXD8 FWD	GGAAGACAAACCTACAGTCGC
HOXD8 REV	TCCTGGTCAGATAGGGGTTAAAA
HOXA9 FWD	TACGTGGACTCGTTCCTGCT
HOXA9 REV	CGTCGCCTTGGACTGGAAG
HOXC9 FWD	ACTCGCTCATCTCTCACGACA
HOXC9 REV	GACGGAAAATCGCTACAGTCC
HOXD9 FWD	GGACTCGCTTATAGGCCATGA

HOXD9 REV	GCAAAACTACACGAGGCGAA
HOXC10 FWD	ACATGCCCTCGCAATGTAACT
HOXC10 REV	GAGAGGTAGGACGGATAGGTG
HOXC11 FWD	ATGTTTAACTCGGTCAACCTGG
HOXC11 REV	GCATGTAGTAAGTGCAACTGGG
HOXD11 FWD	TCTCCGAGTCCTCGTGGGGA
HOXD11 REV	GCAAAACACCAGCGCCTTCTA
HPRT FWD	TCCTTGGTCAGGCAGTATAATCC
HPRT REV	GTCAAGGGCATATCCTACAACAAA